UDK 620.3:661.872.02:615.03
Original scientific article/Izvirni znanstveni članek

ISSN 1580-2949
MTAEC9, 55(4)477(2021)

# QUERCETIN-MODIFIED $Fe_3O_4$ NANOPARTICLE-BASED MEDICAL IMAGING MODALITY FOR THE MONITORING OF THERAPEUTIC-DRUG DELIVERY

## KVERCETINSKO MODIFICIRANI NANODELCI $Fe_3O_4$ ZA SISTEME SLIKOVNEGA OPAZOVANJE IN SLEDENJE DOZIRANJA TERAPEVTSKIH ZDRAVIL

**Ketevan Chubinidze*[1,2], Mariam Kurasbediani[1], Nanuli Doreulee[1], Besarion Partsvania[2], Gia Petriashvili[2]**

[1]Iv. Javakhishvili Tbilisi State University, Faculty of Exact and Natural Sciences, 1 Chavchavadze Ave., Tbilisi 0179, Georgia
[2]Georgian Technical University, Institute of Cybernetics, Zurab Anjaparidze Street 5, Tbilisi 0186, Georgia

*Prejem rokopisa – received: 2021-01-22; sprejem za objavo – accepted for publication: 2021-03-19*

doi:10.17222/mit.2021.017

The combination of imaging and therapeutic agents with drug nanocarriers has received great attention due to the number of outstanding applications in nanobiology and nanomedicine. In this respect, the traditional and biocompatible magnetic nanoparticles, such as $Fe_3O_4$, play a pivotal role, having a versatile potential in imaging diagnostics, treatments and targeting in drug-delivery systems. In this work, we report on $Fe_3O_4$ nanoparticles functionalized with quercetin molecules and show that the conjugation between $Fe_3O_4$ nanoparticles and quercetin significantly modifies the fluorescent properties of the nanocomposite. The obtained results offer a reliable tool for image-assisted drug-delivery systems, targeting and penetrating such a delicate area of the human body as a blood-brain barrier.

Keywords: $Fe_3O_4$ nanoparticles, fluorescence, blood-brain barrier

Nanonosilci dovajanja zdravil, v kombinaciji s slikovnim sledenjem in terapevtskimi posredniki, so v zadnjem času vzbudili veliko pozornosti zaradi številnih možnosti njihove napredne uporabe v nanobiologiji in nanomedicini. Glede na to igrajo tradicionalni in biokompatibilni magnetni nanodelci, kot je $Fe_3O_4$, osrednjo vlogo in imajo velik potencial za izvajanje slikovne diagnostike in obdelave v sistemih za ciljno doziranje zdravil. V pričujočem članku avtorji opisujejo raziskavo uporabe nanodelcev $Fe_3O_4$, funkcionaliziranih s kvercitinskimi molekulami. Avtorji ugotavljajo, da združevanje nanodelcev $Fe_3O_4$ in kvercitina močno spremeni fluorescentne lastnosti nanokompozita. Rezultati raziskave kažejo, da to lahko predstavlja novo učinkovito orodje za slikovno podprte sisteme doziranja zdravil, še posebej v zelo občutljivih primerih, kot je ciljno doziranje in penetracija zdravil v področja človeškega telesa, kot je krvno (žilno) - možganska pregrada.

Ključne besede: nanodelci $Fe_3O_4$, fluorescenca, žilno-možganska pregrada

## 1 INTRODUCTION

The blood-brain barrier (BBB) presents a highly selective anatomical gateway that effectively protects the brain from circulating neurotoxic substances and isolates the peripheral blood from the neural tissue. Conversely, the high barrier function of brain microvascular endothelial cells hinders the ability of neurotherapeutic drugs to exert therapeutic effects in the central nervous system.[1] Tight junctions and adherent proteins prevent paracellular diffusion (i.e., the movement between cells) so that the drugs entering the brain parenchyma must generally cross the luminal and abluminal plasma membranes of the endothelial cells. Drug characteristics that are favourable for crossing the BBB are therefore high lipophilicity, a small size and molecular weight, and low hydrogen-bonding potential.[2] Quercetin (quer.) is a natural bioflavonoid found in vegetables and fruits and is available as a commercial supplement. This molecule possesses many diverse pharmacological activities such as anti-oxidant, anti-inflammatory and anti-cancer functions. However, due to its poor solubility, quercetin was found to be difficult to be absorbed into the body, thus resulting in poor bioavailability in vivo. Fortunately, it was reported that quercetin can form complexes with transition-metal ions, such as $Cu^{2+}$, $Mn^{2+}$ and $Fe^{2+}$.[3,4]

Currently, the most promising and viable drug-delivery system is based on a multifunctional nanoparticle-based delivery platform, where the drug is bound to the nanoparticles capable of crossing the BBB. In recent years, several kinds of nanoparticles combining magnetic and fluorescent properties have been fabricated through the incorporation of superparamagnetic nanoparticles and fluorescent organic dyes or quantum dots. The combination of magnetism and fluorescence in a single nanoparticle provides for a unique applicability that cannot be achieved with conventional materials. For example, the motion of such fluorescent magnetic nanoparticles can be induced by applying an external magnetic field and monitoring it in real-time with fluo-

*Corresponding author's e-mail:
chubinidzeketino@yahoo.com (Ketevan Chubinidze)

rescence measurements.[5,6] In this respect, iron oxide ($Fe_3O_4$) exhibits fascinating physical properties, especially in the nanometer range, not only from the standpoint of basic science but also for a variety of engineering, particularly biomedical applications.[7] In this work, we report on quercetin-modified $Fe_3O_4$ nanoparticles and show that the prepared nanocomposite exhibits a fluorescent emission in the visible range of the optical spectrum, which makes it a promising material for the visualization and tracking of the drug-loaded $Fe_3O_4$ nanoparticles.

## 2 MATERIALS

As the initial substances, we used: an iron oxide, a PEG functionalized, magnetic nanoparticle solution – 1 mg/L of 30-nm-diameter $Fe_3O_4$ dispersion in water, dimethyl sulfoxide (DMSO), which is a polar aprotic solvent that can dissolve a wide range of organic compounds, and 2-(3,4-dihydroxyphenyl)-3,5,7-trihydroxy-4H-1-benzopyran-4-one, 3,3',4',5,6-pentahydroxyflavone (quer.), which promotes and increases the effect of a possible drug delivery, favouring its biological activity. All the aforementioned components were purchased from Sigma-Aldrich.

## 3 EXPERIMENTAL PART

### *3.1 Samples preparation*

In the experiments, we used the above-mentioned initial materials to prepare four solutions in different vials. The first vial was filled with 100 mL of a $Fe_3O_4$/water solution. The second one was filled with 100 mL of DMSO solution, while the third and fourth vials were filled with 100 µL of DMSO/8.3 mg of quer., and 45 µL of DMSO/4.5mg of quer. + 34 µL of $Fe_3O_4$/water, respectively. The as-prepared solutions were strongly stirred at 600 $min^{-1}$ for 2 h at room temperature to avoid the aggregation and to obtain homogeneous solutions. Then a part of each mixture was transferred into a capped quartz cuvette and kept there for 3 h for optical measurements. The isolation of quer./$Fe_3O_4$ nanoparticle conjugates was performed via a centrifugation at 30.000 $min^{-1}$ for 25 min. The obtained nanocomposite was washed three times with ethanol and dried at room temperature for 12 h. After that, the quer./$Fe_3O_4$ nanocomposite was re-dispersed in deionized water for a long-time storage. Note that DMSO is a polar solvent with oxygen and sulphur atoms, playing a vital role as the mediator between quercetin and $Fe_3O_4$ nanoparticles through covalent bonds.

### *3.2 Equipment and optical measurements*

The absorption and fluorescence spectra of the samples were recorded with a fibre-optic spectrometer (Avaspec-2048, "Avantes"). Photoexcitation of the nanomaterials was performed with a nitrogen laser of wavelength 337 nm. As the imaging-based technique was involved, a fluorescence microscope equipped with a high-resolution CCD camera was used. To measure the decay of the fluorescence intensity with time, a photomultiplier tube coupled to an oscilloscope was used. First, using a spectrometer, we measured the absorbance spectra of the composites embedded in the capped quartz cuvettes. **Figure 1** shows the light absorptions of DMSO (a) and $Fe_3O_4$/water solutions (b), while **Figure 2** shows the light absorptions of quer./DMSO (a) and quer./DMSO/$Fe_3O_4$ solutions (b), respectively.

In the second part of the experiments, each solution (i.e., $Fe_3O_4$/water, DMSO, quer./DMSO and quer./DMSO/$Fe_3O_4$), was extracted from the corresponding cuvette and deposited by drop-coating onto glass slides treated with deionized water. The liquid films on the substrates were stored for 48 h at 37 °C. As a result, we obtained aggregations of quer./DMSO and quer./DMSO/$Fe_3O_4$ nanomaterials and showed that quercetin molecules and $Fe_3O_4$ nanoparticles are prone to aggregate into

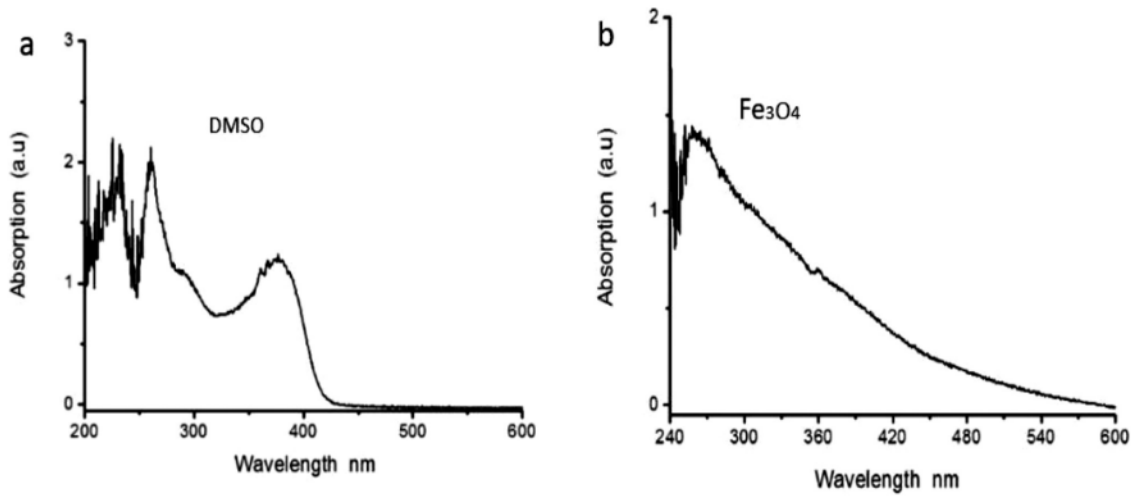


**Figure 1:** a) UV-Visible absorption spectrum of DMSO, b) UV-Visible absorption spectrum of $Fe_3O_4$ nanoparticles dispersed in water

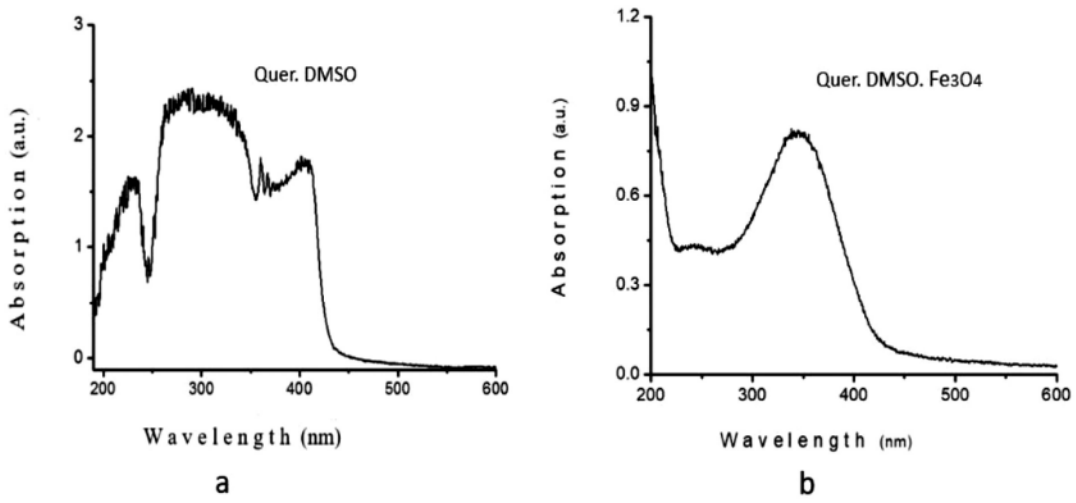


**Figure 2:** a) UV-Visible absorption spectrum of quercetin dissolved in DMSO; b) UV-Visible absorption spectrum of the quer./DMSO/$Fe_3O_4$ nanocomposite

clusters. To investigate the output light intensities, emitted from the clustered composites, we used a laser light source with a wavelength of 337 nm. Fluorescence spectra were recorded using a fibre spectrometer. The experimental set-up used in the study is schematically illustrated in **Figure 3**. A light beam from a nitrogen laser was directed towards the sample at 45° from the normal. The fluorescent emission along the normal forward direction of the sample was collected into a fluorescence microscope, optically coupled with the spectrometer. To visualize the images from different parts of the samples, a high-resolution CCD camera was used.

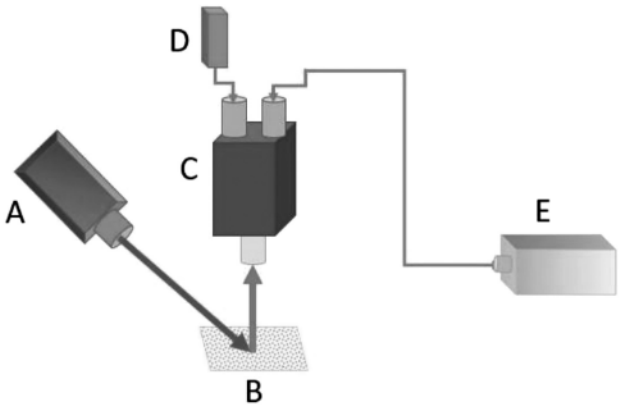


**Figure 3:** Experimental set-up used in this study: nitrogen laser (A), sample (B), fluorescent microscope (C), CCD camera (D), spectrometer (E)

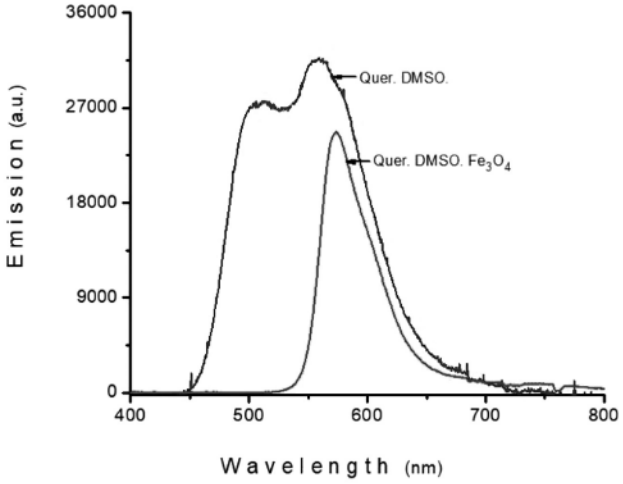


**Figure 4:** Fluorescence emission spectra from quer./DMSO and quer./DMSO/$Fe_3O_4$ composites

**Figure 4** shows the fluorescence emission spectra of the quer./DMSO and quer./DMSO/$Fe_3O_4$ composites. As seen in **Figure 4**, the overall fluorescence intensity from the quer./DMSO/$Fe_3O_4$ nanocomposite was significantly decreased, red-shifted, and narrowing the emission spectral line as compared to the quer./DMSO composite.

## 4 RESULTS AND DISCUSSIONS

To estimate the fluorescence quenching caused by doping $Fe_3O_4$ nanoparticles in the quer./DMSO composite, we used the following Equation (1):[8]

$$Q(\%) = \frac{(F_m - F_n)}{F_m} \times 100\ \% \qquad (1)$$

where, in our case, $Q$ is the percentage of the total fluorescence quenching, $F_m$ is the fluorescence intensity of the quer./DMSO composite and $F_n$ is the fluorescence intensity of the quer./DMSO/$Fe_3O_4$ nanocomposite. To estimate quantitatively the reduction of the fluorescence intensity caused by $Fe_3O_4$ nanoparticles, we, first, calculated the fluorescence intensities of the quer./DMSO and quer./DMSO/$Fe_3O_4$ composites and then calculated the difference between them. In particular, the fluorescence quenching rate can be calculated as follows:

$$Q(\%) = \frac{(F_m - F_n)}{F_m} \times 100\ \% = \frac{\int_{\lambda_m^i}^{\lambda_m^j} F_m(\lambda)\mathrm{d}\lambda - \int_{\lambda_n^i}^{\lambda_n^j} F_n(\lambda)\mathrm{d}\lambda}{\int_{\lambda_m^i}^{\lambda_m^j} F_m(\lambda)\mathrm{d}\lambda} \times 100\ \% \quad (2)$$

Where $\lambda_m^i$, $\lambda_m^j$, $\lambda_n^i$, and $\lambda_n^j$ correspond to the initial and final positions of the wavelength of each graph from **Figure 4**. Using Equation (1), we found that the fluorescence intensity of the quer./DMSO/$Fe_3O_4$ nanocomposite was reduced by 57 % compared to the quer./DMSO composite. According to the Mie theory, small colloids of up to 40 nm in diameter are expected to quench fluorescence because absorption is the dominant mechanism, while larger colloids of above 40 nm are expected to enhance fluorescence because scattering becomes the dominant mechanism.[9] Besides, there are at least two factors that alter the fluorescence properties of a fluorescent dye in the presence of nanoparticles. These include the distance between the fluorescent dye and the nanoparticle, and the orientation of the molecular dipole of the fluorescent dye in relation to the nanoparticle surface. Fluorescence quenching occurs beyond the 10-nm distance limit accepted for the efficient fluorescence resonance energy transfer (FRET) between the donor and quencher molecules.[10–12] The energy transfer efficiency ($E$) was measured using Equation (3) from the lifetime data:

$$E = 1 - \frac{\tau}{\tau_0} \quad (3)$$

where $\tau$ and $\tau_0$ are the lifetimes of the donor in the presence and absence of the acceptor, respectively. To determine a time-resolved luminescence, the luminescence lifetimes of the samples were measured as a function of time after being excited by a beam of light. A pulsed nitrogen-laser light of 3 ns with a wavelength of 337 nm was used to excite the quer./DMSO (i.e., to determine $\tau_0$) and quer./DMSO/$Fe_3O_4$ (i.e., to determine $\tau$) composites. The detector used in this apparatus was a photomultiplier tube coupled to the gigahertz oscilloscope, which displayed the decay of the luminescence intensity with respect to time. The estimated times were $\tau_0 \approx 12 \times 10^{-9}$ s and $\tau \approx 1.36 \times 10^{-9}$ s, respectively. The dependence of the critical donor-acceptor distance ($R_0$), when the energy transfer efficiency is 50 %, on the spectral overlap for a particular donor-acceptor pair is expressed as follows:

$$R_0 = 0.211\left[K^2 \times N^{-4} \times \Phi_0 \times J(\lambda)\right]^{1/6} \quad (4)$$

where $K^2$ represents the relative orientation of the donor to the acceptor molecule. Considering a random rotational diffusion of the small molecules, $K^2$ is taken to be 2/3,[13,14] $N$ is the refractive index of the medium (1.48 for glass/quer./DMSO/$Fe_3O_4$), $\phi_0$ is the quantum yield of the donor in the absence of the acceptor, taken as 0.25, and $J_{(\lambda)}$ is the overlap integral that can be calculated with the numerical integration method using the following relation:

$$J(\lambda) = \frac{\int_0^\infty F(\lambda) \times \varepsilon_A(\lambda) \times \lambda^4 \mathrm{d}\lambda}{\int_0^\infty F(\lambda) \times \mathrm{d}\lambda} \quad (5)$$

Here, $F(\lambda)$ is the luminescence intensity of the donor in a wavelength range of $\lambda$ to $(\lambda + \Delta\lambda)$ with the total intensity normalized to unity while $\varepsilon_A(\lambda)$ is the molar extinction coefficient of the acceptor. For the $Fe_3O_4$ nanoparticles with a size of 30 nm, the molar extinction coefficient is around 3.65 × 106 $M^{-1}$ $cm^{-1}$.[15] The energy-transfer efficiencies from Equation (3) can be rewritten as:

$$E = \frac{R_0^6}{R_0^6 + r^6} \quad (6)$$

Based on the experimental results and calculated data from Equations (3) to (6), we found that the distance between the dye molecules (quer.) and $Fe_3O_4$ nanoparticles, which are statistically on the glass surface, is (14.5 ± 0.60) nm. **Figure 5** shows fluorescent microscopy photographs of the aggregations of quer./DMSO and quer./DMSO $Fe_3O_4$ deposed on glass substrates and

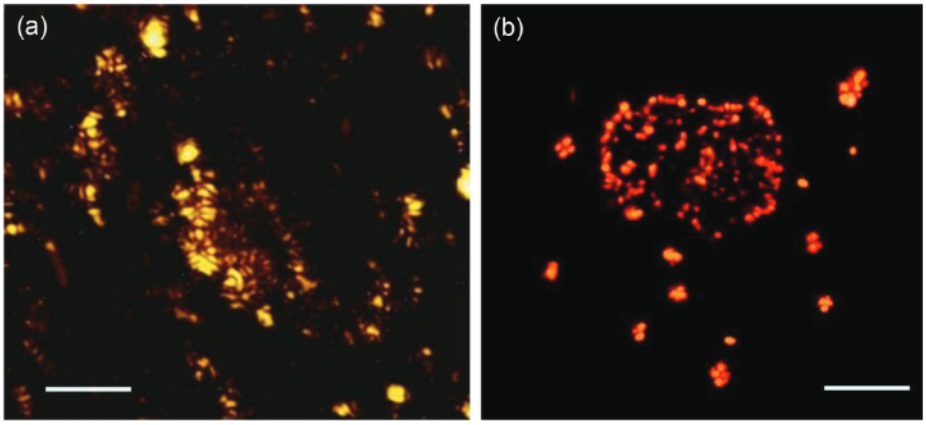


**Figure 5:** a) Fluorescence imaging of self-aggregated quer./DMSO, and b) quer./DMSO/$Fe_3O_4$ composites deposed on glass substrates. The samples were excited with a 337 nm nitrogen laser. The scale bar is 20 μm.

stored at 37 °C for 48 h. Both the quer./DMSO composite and quer./DMSO/ $Fe_3O_4$ nanocomposite tend to self-aggregate.

As seen from the images, the aggregation of the quer./DMSO/$Fe_3O_4$ nanocomposite is red, whereas the quer./DMSO composite appears to be yellowish. We found that the particular properties of the quer./DMSO and quer./DMSO/$Fe_3O_4$ composites, such as fluorescence intensity, colour and graphical profiles of the emissions, make them distinguishable from each other. However, there is a challenge associated with the limited penetration depth of ultraviolet light due to the high scattering and absorption ability of biological tissues. To provide a better penetration ability of light, potentially minimizing the damage of a specimen such as the brain, it is recommended to use the two-photon absorption technique.

## 5 CONCLUSIONS

We prepared and investigated quercetin-modified $Fe_3O_4$ nanoparticles and demonstrated that the functionalization through the conjugation of fluorescent species and magnetic nanoparticles dramatically alters the nanocomposite optical parameters such as fluorescence intensity, spectral position and shape of fluorescence emission. The proposed image-guided drug-delivery system emerges as a promising tool for *in-vivo* tracking of fluorescent dye-labelled therapeutic drugs with functionalized $Fe_3O_4$ nanoparticles in a complicated and delicate biological environment, such as cancer cells and BBB.

### Acknowledgment

This work was supported by the Shota Rustaveli National Science Foundation of Georgia, under project number FR17_629.

## 6 REFERENCES

[1] M. Ohshima, Sh. Kamei, H. Fushimi, Sh. Mima, T. Yamada, T. Yamamoto, Prediction of Drug Permeability Using In Vitro Blood–Brain Barrier Models with Human Induced Pluripotent Stem Cell-Derived Brain Microvascular Endothelial Cells, BioResearch Open Access, 8 (**2019**) 1, 200–209, doi:10.1089/biores.2019.0026

[2] H. V. D. E. Waterbeemd, G. Camenisch, G. Folkers, J. R. Chretienc, O. A. Raevsky, Estimation of Blood-Brain Barrier Crossing of Drugs Using Molecular Size and Shape, and H-Bonding Descriptors, Journal of Drug Targering, 6 (**1998**) 2, 151–165, doi:10.3109/10611869808997889

[3] M. Ersoz, A. Erdemir, S. Derman, T. Arasoglu, B. Mansuroglu, Quercetin-loaded nanoparticles enhance cytotoxicity and antioxidant activity on C6 glioma cells, Pharm. Devel. and Technol., 25 (**2020**) 6, 1097–9867, doi:10.1080/10837450.2020.1740933

[4] Y. Liu, M. Guo, Studies on Transition Metal-Quercetin Complexes Using Electrospray Ionization Tandem Mass Spectrometry, Molecules, 20 (**2015**), 8583–8594, doi:10.3390/molecules20058583

[5] J. H. Lee, Y. W. Jun, S. I. Yeon, J. S. Shin, J. Cheon, Dual-Mode Nanoparticle Probes for High-Performance Magnetic Resonance and Fluorescence Imaging of Neuroblastoma, Angew. Chem. Int. Ed., 45 (**2006**), 8160 –8162, doi:10.1002/ange.200603052

[6] K. M. Yeo, Ch. Ji. Gao, K. H. Ahn, I. S. Lee, Superparamagnetic iron oxide nanoparticles with photoswitchable fluorescence, Chem. Commun., (**2008**), 4622–4624 doi:10.1039/b807462c

[7] D. Shi, M. E. Sadat, A. W. Dunn, D. B. Mast, Photo-fluorescent and magnetic properties of iron oxide nanoparticles for biomedical applications, Nanoscale, The Royal Society of Chemistry, 7 (**2015**), 8209–8232, doi:10.1039/c5nr01538c

[8] M. M. Elsutohy, A. Selo, V. M. Chauhan, S. J. B. Tendlerac, J. W. Aylott, Enhanced distance-dependent fluorescence quenching using size tunable core shell silica nanoparticles, RSC Adv., 62 (**2018**) 8, 35840–35848, doi:org/10.1039/C8RA05929B

[9] H. Ghaforyan, M. Ebrahimzadeh, S. M. Bilankohi, Study of the Optical Properties of Nanoparticles Using Mie Theory, World Appl. Programming, 5 (**2015**) 4, 79–82, ISSN:2222–2510

[10] M. Swierczewska, S. Lee, X. Chen, The design and application of fluorophore–gold nanoparticle activatable probes, Phys. Chem. Chem. Phys., 13 (**2011**) 21, 9929–41, doi:10.1039/c0cp02967j

[11] K. G. Thomas, P. V. Kamat, Chromophore functionalized gold nanoparticles, 36 (**2003**) 12, 888–98, doi:10.1021/ar030030h

[12] K. Chubinidze, B. Partsvania, A. Khuskivadze, P. Burnadze, G. Petriashvili, D. Dzidziguri, O. Mukbaniani, Modeling of Calmodulin-Mediated Processes in Tissues Using Calmodulin-Functionalized Gold Nanoparticles and Fluorescent Dyes, Materials and Technology, 54 (**2020**) 2, 211–214, ISSN 1580-2949

[13] K. Chubinidze, B. Partsvania, T. Sulaberidze, A. Khuskivadze, E. Davitashvili, N. Koshoridze, Luminescence enhancement in nanocomposite consisting of polyvinyl alcohol incorporated gold nanoparticles and Nile blue 690 perchlorate, Applied Optics, 53 (**2014**) 31, 7177–7181, doi:org/10.1364/AO.53.007177

[14] J. R. Lakowicz, Principles of Fluorescence Spectroscopy, 3rd ed., Springer, 2006, 954

[15] X. Zhang, X. Xu, T. Li, M. Lin, X. Lin, H. Zhang, H. Sun, Bai Yang, Composite photothermal platform of polypyrrole-enveloped $Fe_3O_4$ nanoparticle self-assembled superstructures, ACS Appl. Mater. Interfaces, 6 (**2014**) 16, 14552–14561, doi:10.1021/am503831m